

Experimental Investigation on the Pulse Behavior of Polymeric Matrix Composites Used in Vehicles

Hüseyin Bayrakçeken¹, Ercan Şimşir², M. Serhat Başpınar³, İ. Sinan Ath⁴

^{1,2}Afyon Kocatepe University, Faculty of Technology, Automotive Engineering Department, 13200, Afyon / TURKEY

^{3,4}Afyon Kocatepe University, Faculty of Technology, Metallurgy and Materials Engineering Department, 13200, Afyon / TURKEY

Abstract: *The impact load is defined as the momentary force on the material within a very short period of time. The laminated composite materials can be subjected to many impact loads compared to where they are used. In this study, four different types of oriented carbon fiber materials [0°/0°]s, [0°/90°]s, [±45°]s and [0°/90°/+45°/-45°]s were used. Eight-layers aluminum honeycomb carbon fiber/epoxy composite samples cut of 10 cm x 10 cm were made. Four different samples were tested under 80 joule impact energy. Force-slump curves, force-time curves, absorbed energy-time curves and velocity-time curves were plotted. As a result of the experimental study, puncture damage occurred in all the samples exposed to 80 joule impact energy. The material which had the highest damping capacity and maximum strength against the impact was C₄⁸ composite material with eight-layer [0°/90°/+45°/-45°]s. It was concluded that the carrying capacity and impact strength of the C₄⁸ sample were higher than the samples with different fabric orientations. Crush test applied to the carbon fiber/epoxy composite samples and crushing traces, fiber breaks and matrix fractures were observed on the impact applied upper surfaces.*

Keywords: Vehicle, Polymer Matrix Composite, Impact Behavior

1. Introduction

The impacts of composite materials used in many areas such as maritime, aviation, health, sports vehicles and transportation are important, especially in terms of space, aircraft and automobile industry. In this study, the condition of the carbon fiber/epoxy reinforced composite material produced with four different orientation angles when subjected to single pulse energy was investigated experimentally. Damage in the form of a fiber break, matrix crack, delamination and puncture could occur after the impact. Depending on these damages, impact behavior force-slump curves, force-time curves, absorbed energy-time curves and velocity-time curves were formed.

The impact problem of composite materials represents important theoretical and practical applications [1]. The Impact is defined as the instantaneous force on material within a very short period of time. The impacts of the material may vary depending on the intended use and the location of the application [2]. Often the pulses can be classified as high-speed and low-speed. Low-speed impacts range from 1 to 10 m/s [3]. High-speed pulses are the pulses at the ballistic level [4].

The loading type where the composite materials are sensitive is a vertical or perpendicular to the fiber. When the received pulse width is weak in the thickness direction relative to the plane, load-bearing material is reduced and damaged [5].

The impact behavior of composite materials was investigated in many studies. In their study, Belingardi and Vadori investigated the effects of thickness/impact on carbon/epoxy material. The force-displacement graphs were derived by applying dynamic and semi-static impact loading to the samples of different thickness [6]. In their study about laminate composites exposed to low speed impact, Turkmen and Koksall investigated the effect of plate sizes on impact

behavior. In the study, a 180 x 50 mm, 180 x 100 mm and 180 x 150 mm plate was used. They stated that as the width of the material increased, the amount of permanent displacement decreased [7]. They examined the effect of temperature changes on the layer separation of the carbon/epoxy and carbon/peek composite plates at the high and low temperatures in the material and on the matrix crack, and the impacts on the impact using the scanning acoustic microscope (SAM) and optical microscope. They indicated that the separation between layers increased with increasing temperature [8]. They examined the damage of internal structures after repeated impact tests applied to the fiber reinforced composite material. These repetitive impacts indicate that delamination, fiber breakage and matrix fracture damage types occur in the interior of the material [9].

The impact behavior of laminate composite materials was studied and methods were developed. The first study on the dynamic loading behavior of composite materials was made in the early 1970s [10, 11]. Studies in this area have continued with the development of pulse models and research methods [11, 12]. The effects of laminate composite materials on different direction angles, changing the applied impact energy and impact of different layer thicknesses on impact behavior have been investigated [11, 13, 14, 15].

In this study, the impact behavior of carbon fiber/epoxy composite samples with angled angles for constant energy value was investigated experimentally. Honeycomb was used as honeycomb material. For the impact test, the 300 mm x 10 mm carbon fiber / epoxy composite samples vacuum infusion method was used.

Honeycomb structure beams with the same volume supported with carbon fiber fabric with different orientation angles were subjected to three-point bending test, tensile test and impact test and the strengthening effect of carbon fiber/epoxy beam material was investigated. As a result, the reaction of the beams with respect to bending test, tensile test and impact

test conditions was determined. It was found that the C₄⁸ composite material with eight-layers [0°/90°/+45°/-45°]s had higher strength than the other orientations.

2. Material and Method

In the experimental study, eight-layers of 300 mm x 10 mm carbon fiber / epoxy composite plates were used. MGS L285 was used as the resin material and MGS H285 material was used as the hardening material. In each of the 12 test samples produced, 100 grams of epoxy and 40 grams of hardener were used as the resin material. Fiber-epoxy composite fabrics were prepared by the hand lay-up method and eight pieces of resin were applied to the sample material. An aluminum honeycomb piece was placed on the inside of each of the produced samples. The samples were then kept under vacuum for 170 minutes. The samples were produced by hand depositing technique and the vacuum method. Process steps are shown in Figure 1.

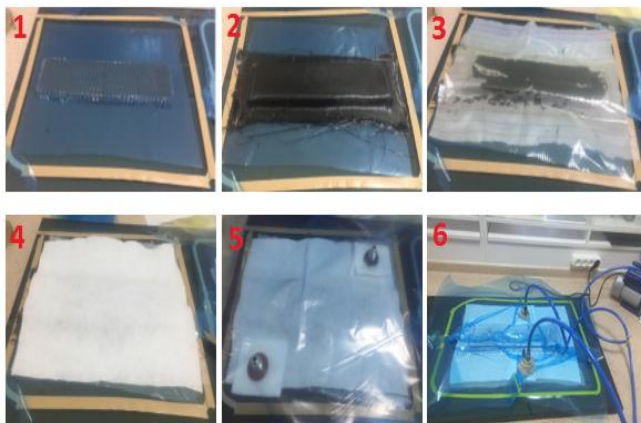


Figure 1: Sample production process steps for impact test

The composite material samples were divided into four groups. Table 1 shows the average layer thickness and layer alignment angles of the composite samples designed as four layers in four groups. In order to compare the angles of alignment layer. C₁⁸, C₂⁸, C₃⁸ and C₄⁸ groups were formed.

Table 1: Grouping and sequencing angles of produced plates

Naming	Layer alignment angles	Average thickness (mm)
C ₁ ⁸	[0°/0°/0°/0°/0°/0°/0°/0°]	2
C ₂ ⁸	[0°/90°/0°/90°/0°/90°/0°/90°]	2
C ₃ ⁸	[+45°/-45°/+45°/-45°/+45°/45°/+45°/45°]	2
C ₄ ⁸	[0°/90°/+45°/-45°/-45°/+45°/90°/0°]	2

Cxy: y: number of layers x: group number

The produced slabs were cut into 10 cm x 10 cm size using WMT3020-DL industrial water jet cutting machine. Impact tests were carried out at room temperature using CEAST 9350 Brand Fractovis Plus falling weight impact tester (Fig 2). The impact mass was 4, 926 kg, and a semi-spherical steel impact tip with a diameter of 12.7 mm was used.



Figure 2: CEAST 9350 (Fractovis Plus) impact tester

The impact test was performed on the samples by means of a pneumatic device in the test device. The samples were exposed to a single energy value of 80 joules. The contact force between the sample and the striker, the amount of sample collapse and the speed of the shooter with time were recorded by Visual impact software. The impact velocity of the striking end of the sample at constant impact energy was C₁⁸, C₂⁸, C₃⁸ and C₄⁸ was 4.98 m/s, 5.44 m/s, 5.37 m/s and 5.20 m/s respectively. Generally three types of damage occur during the impact test; perforation, rebounding and penetration.

As shown in the Figure 3, the curve has a parabolic shape in low-energy pulses (eg the rebounding curve). The generated force increases by the increase of the impact energy. The maximum forces reach the same value for penetration and perforation curves. In order for the force to be zero, the puncture must occur in the sample. However, the tip of the curve runs parallel to the horizontal axis due to friction between the specimen and the striker.

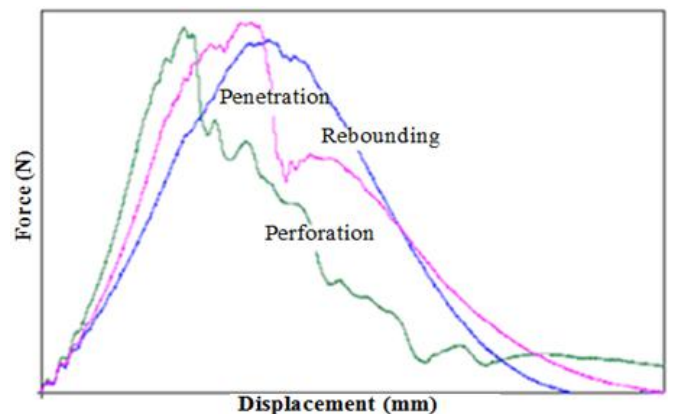


Figure 3: Force - displacement curve [17].

The curve is divided into open type and closed type curve with the increase of pulse energy. The closed type curve is the curve formed by the back tab of the shooter after the impactor applies a pulse to the test sample. That is, part of the impact energy was absorbed by the sample, and the non-absorbable energy was used for the back tab (Fig 3). With the increase of the impact energy, the closed curve decreases and the collapse increases as the back tab decreases. When the

curve is open, the striker tip is punctured or inserted into the sample. Thus, the striker that enters the specimen moves down the thickness of the sample and the back-tab does not occur. When the energy is increased, the striker tip is inserted into the sample, moves during the thickness of the sample and exits from the bottom by puncturing the sample, ie puncture occurs. The end portions of the curves closing towards the end of the horizontal axis refer to the friction between the impactor and the sample. Thus, increasing the impact energy, it is understood that the composite material will not dampen more impact energy [16, 17].

The energy-time (Ea-t) curves absorbed during the impact tests are one of the graphs used to determine the impact behavior of the composite material during the impact event. In the case of low-speed impact tests, when the striker is tabbed back from the sample surface, the energy of the striker can be swallowed by the sample and the non-swallow pulse energy is consumed for the tab of the shooter from the sample surface. At the end of the impact event, the amount of energy that passes from the shooter to the composite sample increases to the energy that causes the most damage to the composite sample. Figure 4 also increases, as shown before each curve then falls from the maximum value reached and then follows a horizontal path at a constant value. This gives the maximum point of pulse energy (Ei) achieved. The fixed point reached in the horizontal absorbed energy (Ea). The difference between the two rebound energy (Er). [18].

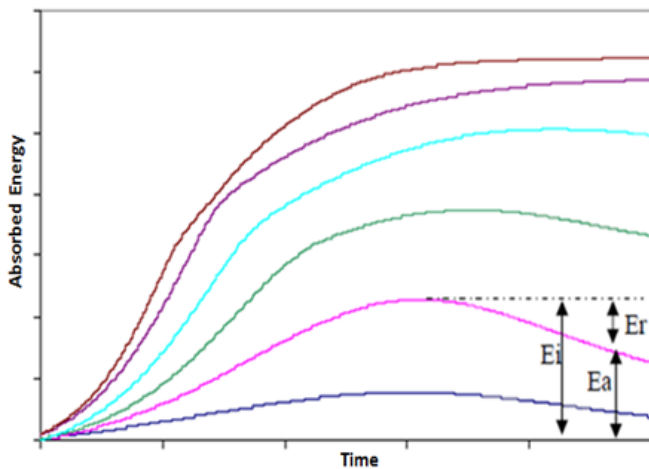


Figure 4: Absorbed energy-time (Ea-t) curve [18].

3. Results and Discussion

3.1 Force - Slump Curves

80 joule energy impact tests were performed for eight-layers of composite samples with four different layers. According to the data obtained as a result of the experiments C_1^8 , C_2^8 , C_3^8 and C_4^8 groups were drawn to the strength slump curve (Fig 5).

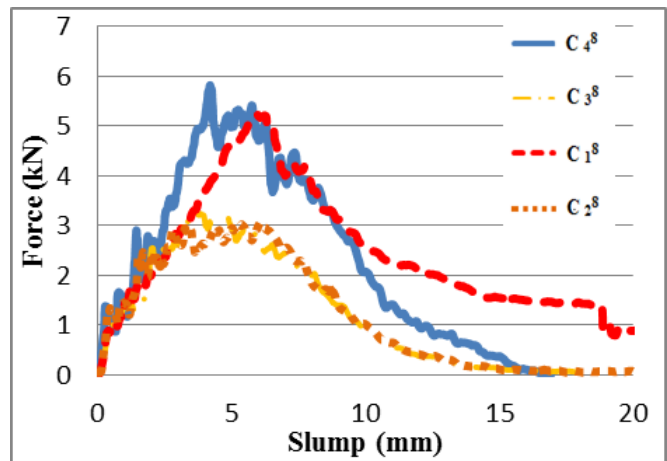


Figure 5: Force-Slump curve of eight-layered composite samples with four different layer sequences

When the force-slump curve given in Figure 5 is examined, it is seen that the samples of C_1^8 , C_2^8 , C_3^8 and C_4^8 show a similar impact behavior for the 80 joule impact energy value. For each of the four groups, the open curve was formed at 80 joule pulse energy values. The reason for the absence of closed curves was due to the high impact energy value and the failure of the striker. Puncture occurred in samples with an open curve. It is seen in Figure 5 that the C_4^8 group sample having $[0^\circ/90^\circ/+45^\circ/-45^\circ]$ layer sequence for the 80 joule impact energy value across all layer sequences carries more maximum force than the other groups.

3.2 Energy - Time Curves

In the energy-time curves, the whole energy is not swallowed by the sample in the event that the striker tip is tabbed back from the sample surface. In this case, the swallow pulse energy is consumed for the back tab of the striking tip from the sample surface. In the event that the beating end is inserted into the sample, the impact energy of the hitter is all swallowed by the sample. In the penetration of the sample from the penetrating tip, the curve is directed upward by the addition of the amount of energy ingested by the impact device in the area under the friction curve between the sample and the striker [11, 17].

The energy-time curves of the eight-layer C_1^8 , C_2^8 , C_3^8 and C_4^8 sequences under constant impact energy are given in Figure 6. The C_1^8 , C_2^8 , C_3^8 , C_4^8 of curve 80 joule impact energy value for the sample is directed upwardly and puncture occurred because rebound from the sample surface did not occur. Since the C_1^8 sample had a unidirectional fiber alignment, the puncture did not occur immediately, but it was not preferred because of serious damage to the sample. This can be seen in Figure 9 according to other samples. Hence, the C_4^8 sample has absorbed energy more than other groups.

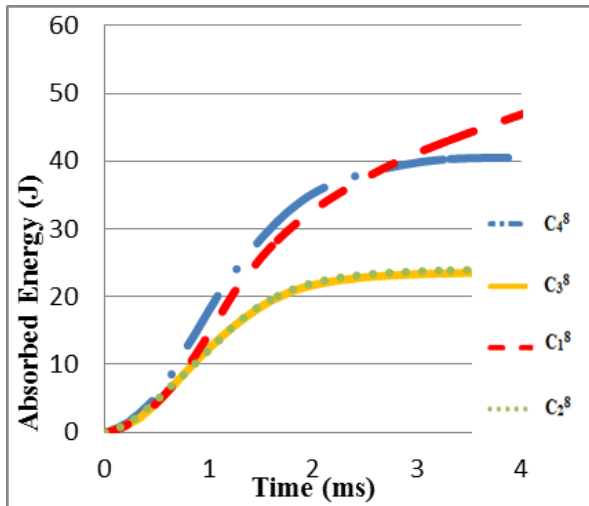


Figure 6: Energy - time curve of eight-layered composite samples with four different layer sequences.

Impact velocity, absorbed energy, surface damage and contact time for each type of material are given in the Table 2. It is seen that the C_4^8 sample absorbs excess energy compared to the other samples. However, the surface damage has undergone a lot of deformation in the upper and lower surfaces as shown in Figure 9 when compared to the other samples. Therefore, separation and tearing are undesirable damages of the composite materials which are used in the automotive industry. Thus, the C_4^8 sample absorbed energy and the top-bottom surface damage was the best result.

Table 2: Impact velocity of sample, absorbed energy, surface damage and contact time

Applied Pulse Energy (J)	Material type	At the time of the crash Speed (m/s)	Absorbed Energy (J)	Surface Damage Width (mm)	Contact Time (s)
80 Joule	C_4^8	5, 2008	40, 5400	12	0, 0007716
	C_3^8	5, 3847	24, 1386	15	0, 0006766
	C_1^8	4, 9871	50, 9952	69	0, 0011141
	C_2^8	5, 4503	26, 1532	14	0, 0004808

3.3 Slump - Time Curves

Figure 7 shows the slump-time curves of samples C_1^8 , C_2^8 , C_3^8 and C_4^8 with different sequence angles. Puncture occurred in all of the samples C_1^8 , C_2^8 , C_3^8 and C_4^8 under 80 joules of impact energy (Figure 7). Slump of the C_4^8 sample having $[0^\circ/90^\circ/+45^\circ/-45^\circ]$ s sequence at 80 joule energy level was lower than the C_2^8 sample with $[0^\circ/90^\circ/0^\circ/90^\circ]$ s sequence and C_3^8 sample with $[+45^\circ/-45^\circ/+45^\circ/-45^\circ]$ s sequence and higher than the C_2^8 sample with $[0^\circ/90^\circ/0^\circ/90^\circ]$ s in sequence. The largest crash occurred in the C_3^8 sample with precipitation occurring.

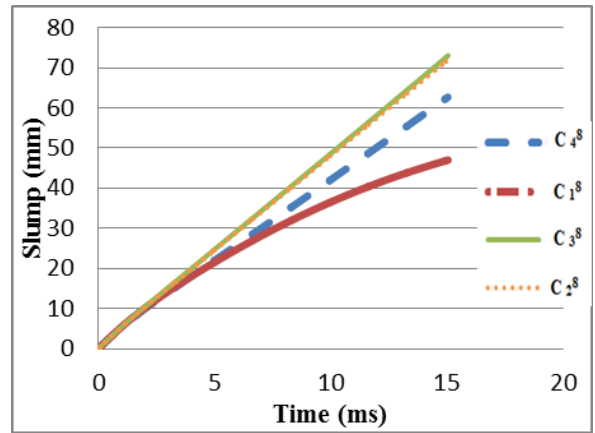


Figure 7: Slump-time curves of eight-layered samples with different orientation angles.

3.4 Velocity -Time Curve

In Figure 8, the velocity of the tracer traveling along the thickness after contacting the sample with constant velocity at 80 joules of impact energy for the eight-layers C_1^8 , C_2^8 , C_3^8 and C_4^8 samples was slowed by friction. Thus, the backbone did not occur and it showed puncture behavior in four samples. If the impact energy was lower, the speed of the shooter with a constant velocity, after contact with the samples, would decrease, and a backlash would occur with the upward moving shooter receiving a negative speed value [11].

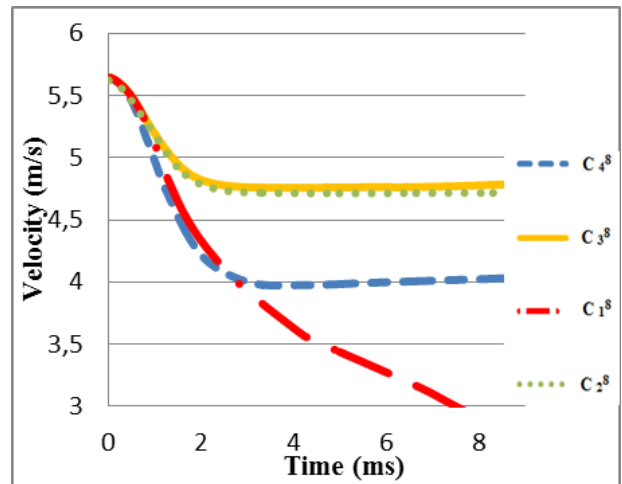


Figure 8: Speed-time curves of eight-layered samples with different orientation angles

In the case of layered composite materials, damage to the matrix is caused by impact on the upper surface. Damage to the matrices starts with the crack and causes the fracture to break. By overloading the matrices, stresses are transferred to the fibers and they start to be strained. This causes matrix breaks to begin in the separation of layers. When the upper layers are broken and cracks reach the interface, they are stopped by the other layer and separations begin between the layers. Separations between layers are not between the layers in the same layer team, but between the layers with different fiber orientations. The bending stiffness of the layers varies according to the different orientations between the layers in the laminated composites. The reason for the separation between layers is the bending rigidity difference between the

sheet and the bending-induced stress. The greater the discrepancy between this bending stiffness, the greater the separation area between layers [5, 11].

As a result of the impact, the cutting and compression stresses on the layers on the upper surfaces cause breakage in the matrix and lead to separation between the layers in the interior of the composite. Separation of vertical bending fractures in the inner region of the composite starts at the lower interface. Bending stresses that occur at the layers on the lower surfaces break the matrix and fiber interface due to bending and fractures occur in the fiber and matrix. On the lower surfaces, matrix and fiber fracture increases and puncture occurs due to the high tensile stresses from bending and high tensile elongation on the surface fibers.

Figures 9 and 9.1 show the damage of the eight-layer C_1^8 , C_2^8 , C_3^8 and C_4^8 samples on the upper and lower surfaces after the impact. It is clear from the figure that the damage zone occurring in samples with different orientation sequences under constant impact energy is evident. In the, C_2^8 and C_3^8 samples, when the post-impact damage zones for 80 joules were compared, it was seen that the lower and upper surface damage regions of these two samples were the same. Under the same energy, the C_4^8 sample has a smaller damage area than the others on the upper surfaces. However, in the C_1^8 sample, it is seen that the upper and lower surfaces have tear and separation in the fiber direction. Therefore, since the separations and tears are undesirable between the layers of the carbon fiber material, this orientation type will not be preferred. Since sample C_2^8 $[0^\circ/90^\circ/0^\circ/90^\circ/0^\circ/90^\circ/0^\circ/90^\circ]$ is in the array, the intermediate part of the composite consists of two layers having the same directional carbon fibers and has a greater resistance to bending by the impact. In C_4^8 sample with $[0^\circ/90^\circ/+45^\circ/90^\circ/45^\circ/+45^\circ/90^\circ/0^\circ]$, the response of the C_4^8 sample to the impact is more than C_2^8 it is low.

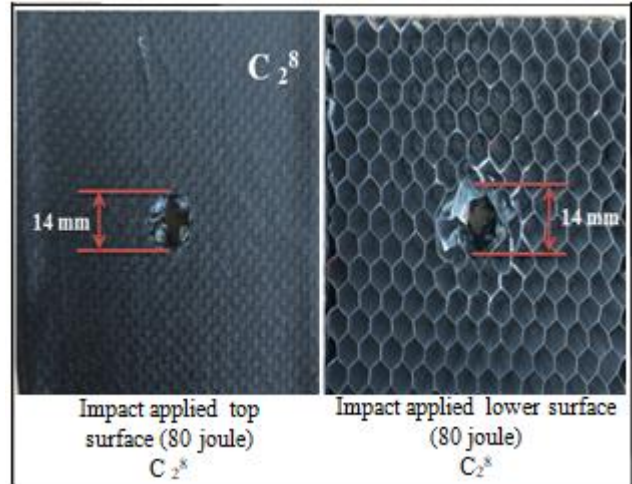


Figure 9: Photos of the upper and lower surface damage zone after the impact of samples with C_1^8 and C_2^8 sequences for constant joule value

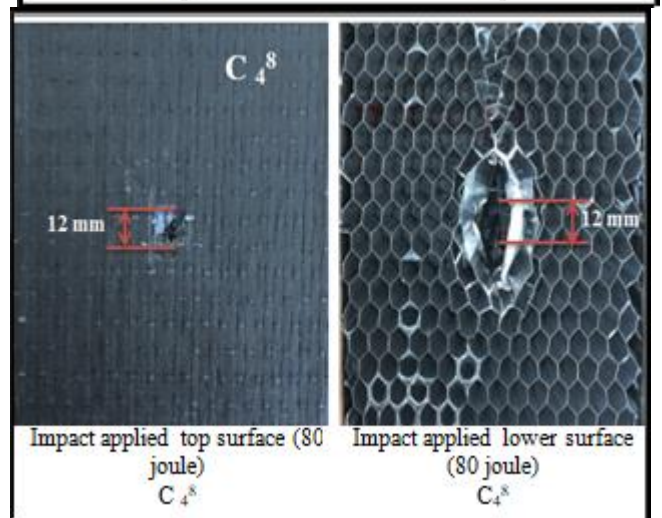
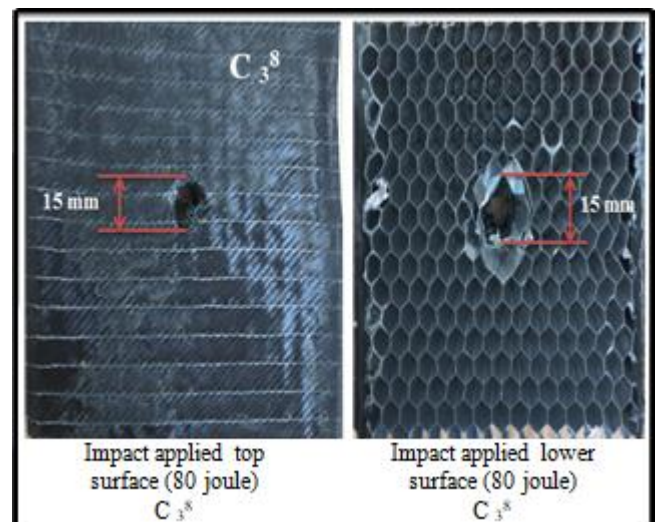
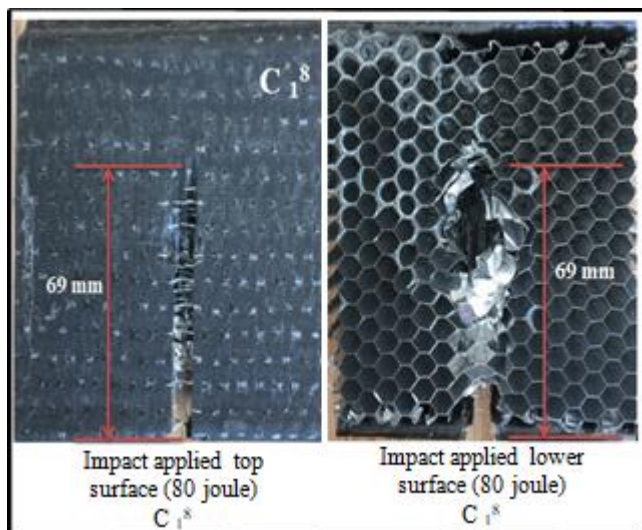


Figure 9.1 Photographs of the upper and lower surface damage area after the impact of samples with C_3^8 and C_4^8 sequences for constant joule value.



Figures 9 and 9.1 show the damage zone photographs of the top and bottom surfaces of the samples with eight-layers samples under constant impact energy. As can be seen from the figure 9, it is seen that the sample having C_1^8 sequence for the 80 joule energy level has crashes and separations in the

carbon fiber material on the impacted upper surface and there are collapse and puncture. Samples with C_2^8 and C_3^8 sequences for the 80 joule energy level are seen to have impact and puncture on the impacted upper surface of the carbon fiber material. For the 80 joule energy level, it is seen that there are damage and perforation on the surface of the impacted upper surface of the specimen with a C_4^8 array on the carbon fiber material. For the 80 joule energy level, the width of the damaged area on the upper surfaces was found to be 69 mm in the C_1^8 sample, 14 mm in the C_2^8 sample, 15 mm in the C_3^8 sample and 12 mm in the C_4^8 sample. As a result, it is seen that carbon fiber material decreases in width and pitting of the damage zone as a result of constant energy.

4. Conclusion

The experimental results in the constant power under a carbon fiber/epoxy composite material that they affect different fiber orientation on impact behavior were investigated and the following results were obtained.

- The deformation area on the impacted upper surface was found to be larger than the deformation area at the unblocked lower surface.
- In all eight-layer C_1^8 , C_2^8 , C_3^8 and C_4^8 samples, an open curve of 80 joules of energy was formed.
- Eight-layers having different orientation angles C_1^8 , C_2^8 , C_3^8 and C_4^8 samples showed similar behavior under constant impact energy. In order to determine the maximum forces and the amount of slump in the eight-layered samples, the sequence was $C_3^8 > C_2^8 > C_4^8 > C_1^8$.
- The maximum crash pulse energy was measured at $[+45^\circ/-45^\circ/+45^\circ/-45^\circ/+45^\circ/-45^\circ/+45^\circ/-45^\circ]$ combination with the C_3^8 sample, and a minimum sag was at $[0^\circ/0^\circ/0^\circ/0^\circ/0^\circ/0^\circ/0^\circ/0^\circ]$ in combination with C_1^8 sample at 80 joule.
- Puncture damage occurred because of the increased breakage of matrix and fiber material on the non-impacted surface of the composite sample. The excessive tensile stress due to bending, and the breaks at the surface fibers were the main reason of such a failure.
- Breakage of the matrix cracks and enlargement of the failure zone were observed in carbon fiber/epoxy composite samples at the 80 joules of energy. It has been observed that the impact energy on the lower surface and damaged area at the lower surface were further enlarged, and perforation was occurred by the simultaneous breaking of fibers at the outer surface and matrix.

5. Nomenclature

[]s symmetry of composite material

C_1^8 Eight-layer $[0^\circ/0^\circ/0^\circ/0^\circ/0^\circ/0^\circ/0^\circ/0^\circ]$ oriented composite material.

C_2^8 Eight-layer $[0^\circ/90^\circ/0^\circ/90^\circ/0^\circ/90^\circ/0^\circ/90^\circ]$ oriented composite material.

C_3^8 Eight-layer $[+45^\circ/-45^\circ/+45^\circ/-45^\circ/+45^\circ/-45^\circ/+45^\circ/-45^\circ]$ oriented composite material.

C_4^8 Eight-layer $[0^\circ/90^\circ/+45^\circ/-45^\circ/-45^\circ/+45^\circ/90^\circ/0^\circ]$ oriented composite material.

J joule

Thanks

The experimental studies were carried out with the budget provided by the 17 FEN. BIL. 65 BAP project.

References

- [1] Uyaner, M., Kara, M., Ataberk, N., E Camı/Epoksi Tabakalı Kompozitlerin Düşük Hızlı Darbe Davranışına Numune Boyutlarının Etkisi. 8. Uluslararası Kırılma Konferansı Bildiriler Kitabı. 7-9 Kasım, İstanbul, 361-368, (2007).
- [2] Kara, M., Düşük Hızlı Darbe Sonrası Yama ile Tamir Edilmiş Filaman Sarım CTP Boruların İç Basınç Altındaki Hasar Davranışı. Selçuk Üniversitesi, Fen Bilimleri Enstitüsü, Doktora Tezi, 126s, Konya, (2012).
- [3] Mili, F., Necib, B., Impact Behavior of Cross-Ply Laminated Composite Plates Under Low Velocities. Composite Structures, 51, 273-244, (2001).
- [4] Jenq, S.T., Mo, J.J., Ballistic Impact Response for Two-Step Braided Three Dimensional Textile Composites. American Institute of Aeronautics and Astronautics, 34 (2), 375-384, (1996).
- [5] Ceyhun, V., Turan, M., Tabakalı Kompozit Malzemelerin Darbe Davranışı. Mühendis ve Makine, 44 (516), 35-41, (2003).
- [6] Belingardi, G., Vadori, R., Low Velocity Impact Tests of Laminate Glass- Fiber Epoxy Matrix Composite Material Plates. International Journal of Impact Engineering, 27, 213-229, (2003).
- [7] Türkmen, İ., Köksal, N.S., Cam Elyaf Takviyeli Polyester Matrisli Kompozit Malzemelerde (CTP) Elyaf Tabaka Sayısına Bağlı Mekanik Özelliklerin ve Darbe Dayanımının İncelenmesi, Celal Bayar Üniversitesi, Fen Bilimleri Dergisi, 8(2): 17-30, (2013).
- [8] Im, K.H., Cha, C.S., Kim, S.K., Yang, I.Y., Effects of Temperature on Impact Damages in CFRP Composite Laminates, Composites: Part B., 32, 669-682, (2001).
- [9] Fidan, S., Avcu, E., Sınmazçelik, T., Cam Fiber Takviyeli Polyester Kompozitte Tekrarlı Darbe Yüklemeyle Oluşan Hasar Mekanizmaları, I. Ulusal Ege Kompozit Malzemeler Sempozyumu, 17-19 Kasım, İzmir, 1-12, (2011).
- [10] Sierakowski, R.L., Nevil, G.E., Ross, A. Jones, E.R., Dynamic Compressive Strength and Failure of Steel Reinforced Epoxy Composites. Journal of Composite Materials, 5, 362-377, (1971).
- [11] Öndürücü A., Karacan A., Tabakalı Cam Elyaf/Epoksi Kompozitlerin Darbe Davranışının Deneysel Olarak İncelenmesi, Mühendislik Bilimleri ve Tasarım Dergisi, 6(3), 435 – 447, (2018).
- [12] Sierakowski, R.L. and Chaturvedi, S.K., Dynamic Loading and Characterization of Fiber-Reinforced Composites. New York, Wiley, (1997).
- [13] Hosur, M.V., Adbullah, M., Jeelani, S., Studies on the Low-Velocity Impact Response of Woven Hybrid Composites. Composite Structures, 67, 253-262, (2005).
- [14] Kessler, A., Bledzki, A.K., Low Velocity Impact Behavior of Glass/Epoxy Cross-Ply Laminates with Different Fiber Treatments. Polymer Composites, 20 (2), 269-278, (1999).

- [15] Datta S., Krishna, A. V., Rao, R. M. V. G. K., Low Velocity Impact Damage Tolerance Studies on Glass-Epoxy Laminates-Effects of Material, Process and Test Parameters. Journal of Reinforced Plastics and Composites, 23 (3), 327-345, (2004).
- [16] Yıldızhan, İ., Hibrit Kompozit Malzemelerin Darbe Davranışı. Süleyman Demirel Üniversitesi, Fen Bilimleri Enstitüsü, Makine Mühendisliği Anabilim Dalı, Yüksek Lisans Tezi, 83s, Isparta, (2013).
- [17] Sayer, M., Hibrit Kompozitlerin Darbe Davranışlarının İncelenmesi. Pamukkale Üniversitesi, Fen Bilimleri Enstitüsü, Doktora Tezi, 134s, Denizli, (2009).
- [18] Akgün, Y., Onarılmış Kompozit Plakların Darbe Davranışları, Yüksek Lisans Tezi, Dokuz Eylül Üniversitesi Fen Bilimleri Enstitüsü, İzmir, (2010).

Author Profile



Hüseyin Bayrakçeken, between 1988-1993 he completed his education on machinery. Between 1995-1998, he completed his master's degree in machine training. He completed his doctorate in the field of mechanical education between 1998-2002. He is currently working as a professor in automotive engineering department.



Ercan ŞİMŞİR, between 2008-2012, he graduated as a machine drawing and construction teacher. Between 2013-2016 he completed his master's degree in mechanical engineering. As of 2016, he is doing his PhD in automotive engineering. He works as a lecturer at the university.



M. Serhat Başpınar, graduated from the metallurgical and materials engineering department between 1988-1993. Between 1994 and 1996, he completed his master's degree in the department of ceramic engineering. He completed his doctorate in the Department of Ceramic Engineering between 1999-2005. He currently works as an associate professor in the department of metallurgy and materials engineering.



İ. Sinan Atlı, between 2003-2008 he graduated from materials science and engineering department. Between 2010-2012, he completed his master's degree at New South Wales University. As of 2013, he is working as a doctor in materials science and engineering department. He is currently working as a research assistant at the Faculty of Technology.